Steel and Composite Structures, Vol. 3, No. 5 (2003) 307-320
DOI: http://dx.doi.org/10.12989/scs.2003.3.5.307

Sway buckling of down-aisle, spliced, unbraced pallet rack structures

R.G. Beale† and M.H.R. Godley‡

Slender Structures Research Group, OCSLD Technology
Oxford Brookes University, Gipsy Lane, Headington, Oxford, UK

(Received March 4, 2003, Accepted July 29, 2003)

Abstract. This paper presents an efficient approach to the determination of the buckling loads of down-aisle, spliced, unbraced, pallet rack structures subjected to vertical and horizontal loads. A pallet rack structures is analysed by considering the stability equations of an equivalent free-sway column. The effects of semi-rigid beam-to-upright, splice-to-upright and base-plate-to-upright connections are fully incorporated into the analysis. Each section of upright between successive beam levels in the pallet rack is considered to be a single column element with two rotational degrees of freedom. A computer algebra package was used to determine modified stability equations for column elements containing splices. The influence of the position of splices in a pallet rack is clearly demonstrated.

Key words: cold-formed steel; pallet racks; design; stability; buckling.

1. Introduction

Pallet rack structures are used in factories and warehouses for the storage of palletised goods. Such structures often have a large number of bays and beam levels. The racks are usually made from cold-formed steel and the sections are in shapes such as channels and hat sections (Yu 1973). The connections between base-plates and uprights and between uprights and beams are usually semi-rigid. A typical example of such a structure is shown in Fig. 1.

With increasing experience in use this type of structure is being constructed with more storeys and greater storey heights. As the rack gets higher it is often necessary to include splices in the uprights as the lengths of uprights required can not be manufactured and processed in one piece and also for efficient design upright sections can be varied throughout the height of the rack. Fig. 2 shows the front and rear views of a splice in a section of upright.

In the design of such structures consideration must be given to the elastic stability of the racks. Previous investigations into rack stability have been made by several authors. Davies (1980, 1992) analysed the down-aisle stability by considering a single upright model carrying both vertical and horizontal loads. His model took into account semi-rigid joints between beams and uprights as well as at the base of the rack. However, the model allowed for column flexibility only below the second beam level. As racks become more slender this approximation becomes less accurate. Lewis (1991) produced

†Principal Lecturer
‡Senior Research Fellow

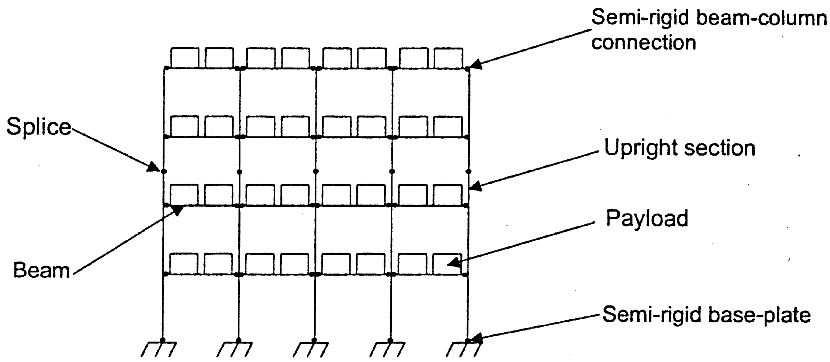

Fig. 1 Typical beam and column arrangement

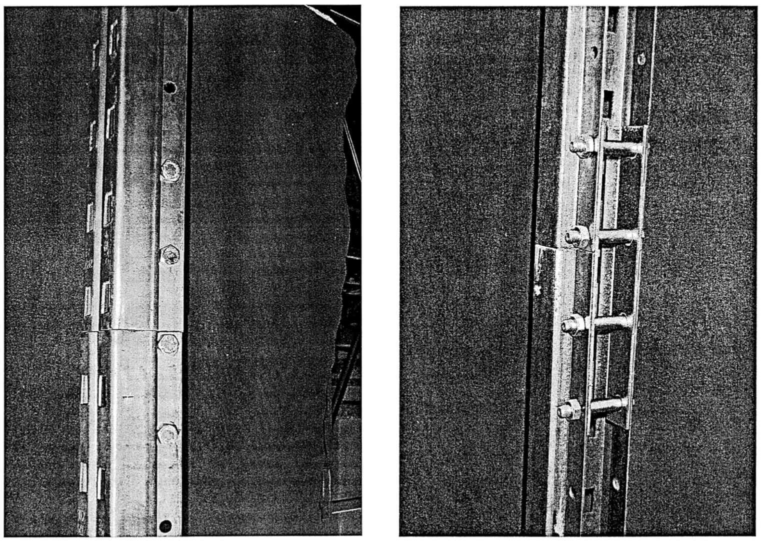

(a) Side view (b) Rear view

Fig. 2 Side and rear views of a splice connection

a simple rigid plastic model for a rack with pinned connections at the base which also assumed that bending distortion within the upright was negligible. In practice, pallet rack structures are more complex and often fail due to elastic instability. McConnel and Kelly (1983) investigated progressive collapse of rack structures but did not report on their analytical model, concentrating on the mode of collapse. The latest code by the Federation Europeanne de la Manutention (2000) requires a second order non-linear analysis to be undertaken in the design of the structures. The code also requires that splices are treated as semi-rigid joints.

The authors in a series of papers (Beale and Godley 2001, Godley *et al.* 1993, 2000) have developed a single column model which accurately predicts the behaviour of regular pallet racks subjected to horizontal and vertical loads. However, in common with all simplified models known to the authors, the original model is unable to analyse structures containing splices in the uprights. This paper derives the revised stability equations for this case and discusses the influence splices have upon the overall stability of the rack structure.

2. Structural model

2.1. Introduction

The beam-upright pallet-rack system shown in Fig. 1 can be treated as a free sway structure with uniform loads acting on the beams. Pallet rack systems normally consist of many bays, each identically loaded, with the same beams and upright sections at corresponding levels throughout the frame. A single column structural model can therefore be used to analyse the rack. The loads from the beams can be equivalently applied to the centre of the line of the upright as a concentrated load. The rotational stiffness of the upright due to the beams can be represented by a rotational stiffness of the beam-to-upright joints. A single column structural model for this unbraced framework is given in Fig. 3, where k_0 and k_i (i = 1,2,.., n) are the rotational stiffnesses of the semi-rigid upright-base-plate and beam-to-upright joints respectively. k_{splice} represents the rotational stiffness of a splice. There can be several splices in an upright. It is assumed that all uprights in a pallet rack are spliced at the same vertical heights.

Because a pallet rack structure can be considered to be a multi-bay framework with no sway bracing, the likely deformed shape is given in Fig. 4. Beam-to-upright joints in rack structures are of many types (Markazi *et al.* 1997). For cold-formed steel members, the joints are often formed by hooks and slots (see Fig. 5). Due to the lack of symmetry at each end of the beam these joints often have different rotational characteristics between the left and right ends which implies that $k_{ri} \neq k_{li}$. Examples of the lack of symmetry are found in Markazi *et al.* (1997) with regard to up-welded and down-welded connectors.

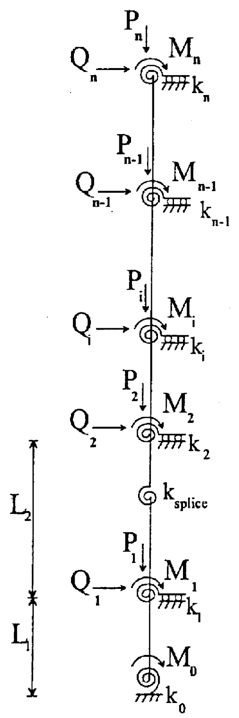

Fig. 3 Structural model

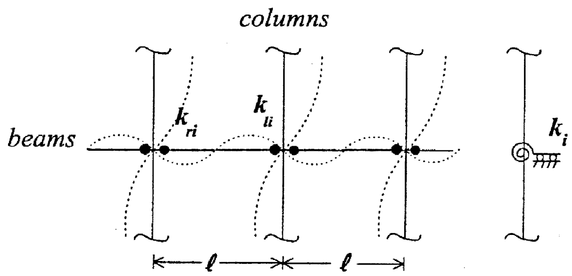

Fig. 4 Equivalent beam-to-upright rotational stiffness

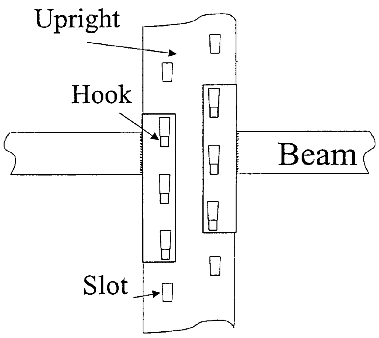

Fig. 5 Typical beam-to-upright connection

The rotational stiffness of a joint is defined as the bending moment required per unit rotation. This implies that at joint i the equivalent beam-to-upright stiffness can be shown to be

$$k_i = \frac{1}{\dfrac{l}{12EI_{bi}} + \dfrac{1}{4k_{li}} + \dfrac{1}{4k_{ri}}} \tag{1}$$

where l is the width of each bay in the rack, I_{bi} the second moment of area of the beam at level i, and k_{li} and k_{ri} the rotational stiffnesses of the beam-to-upright joints. E is Young's Modulus of Elasticity. In the limit as the values of k_{li} and k_{ri} approach infinity then the equivalent beam rotation stiffness is

$$k_i = 12\frac{EI_i}{l} \tag{2}$$

Base-plates are attached at the base of the uprights. The base-plate may, or may not, be bolted to the floor which is usually concrete. The base-plate behaviour is modelled by the base-plate rotational stiffness k_0. This stiffness is determined experimentally and described by Godley *et al.* (1998). It has to be noted that the stiffness is dependent upon the axial load in the column.

The above assumptions require the joints to exhibit their full rotational stiffness immediately. In practice, many joints exhibit highly non-linear moment-curvature relationships including initial states of zero moment or looseness. The authors' experience is that this initial zone increases the deflections in the structure but, provided the magnitude of the looseness is small, the effect on elastic buckling is small. Therefore the assumptions above are adequate for design purposes.

2.2. Derivation of the stiffness equations

The general structural model shown in Fig. 3 will be applied to all regular pallet rack structures. To determine the buckling load of the sway structure the shear forces applied to the rack have to be zero. In this case the standard slope deflection equations for an element without a splice are

$$M_{ab} = i_{ab}\theta_a \frac{\nu}{\tan\nu} - i_{ab}\theta_b \frac{\nu}{\sin\nu} \tag{3}$$

and

$$M_{ba} = -i_{ab}\theta_a \frac{\nu}{\sin\nu} + i_{ab}\theta_b \frac{\nu}{\tan\nu} \tag{4}$$

(Horne & Merchant 1965) where M_{ab} and M_{ba} are the bending moments at each end of the element. θ_a and θ_b are the corresponding rotations at each end of the element. $i_{ab} = \frac{EI}{L}$ and $\nu = \sqrt{\frac{P}{EI}}\,L$ where EI is the flexural rigidity of the element and P the axial load within the element.

Fig. 6 shows a single column element of length L containing a splice distance L_1 from the left hand end. The rotational stiffness of the splice is k_{splice} and the moments on either side of the splice connection are respectively M_1 and M_2.

The corresponding slope deflection equations for the two upright segments are

$$M_{ab} = i_1\theta_a \frac{\nu_1}{\tan\nu_1} - i_1\theta_1 \frac{\nu_1}{\sin\nu_1} \tag{5}$$

$$M_1 = -i_1\theta_a \frac{\nu_1}{\sin\nu_1} + i_1\theta_1 \frac{\nu_1}{\tan\nu_1} \tag{6}$$

for the sub-element below the splice, and

$$M_2 = i_2\theta_2 \frac{\nu_2}{\tan\nu_2} - i_2\theta_{ba} \frac{\nu_2}{\sin\nu_2} \tag{7}$$

$$M_{ba} = -i_2\theta_2 \frac{\nu_2}{\sin\nu_2} + i_2\theta_{ba} \frac{\nu_2}{\sin\nu_2} \tag{8}$$

for the sub-element above the splice, where θ_1 and θ_2 are the rotations on either side of the splice.

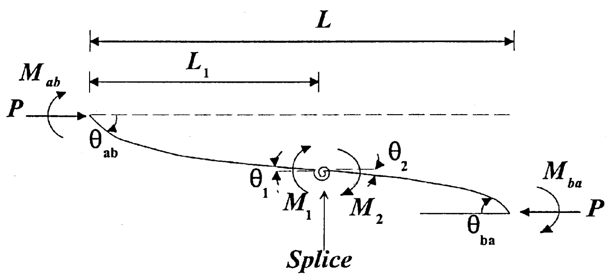

Fig. 6 Column element containing splice

In this case $i_1 = \dfrac{EI_1}{L_1}$, $i_2 = \dfrac{EI_2}{L - L_1}$, $\nu_1 = \sqrt{\dfrac{P}{EI_1}}L_1$ and $\nu_2 = \sqrt{\dfrac{P}{EI_2}}(L - L_1)$

I_1 and I_2 are the second moments of area on the column elements on the two sides of the splice.

Splice continuity requires that

$$M_1 + M_2 = 0 \tag{9}$$

$$\theta_1 - \theta_2 = \frac{M_2}{k_{splice}} = -\frac{M_1}{k_{splice}} \tag{10}$$

Eqs. (5)-(10) contain the variables M_{ab}, M_{ba}, M_1, M_2, θ_{ab}, θ_{ba}, θ_1 and θ_2. The standard slope deflection Eqs. (3) and (4) contain only M_{ab}, M_{ba}, θ_{ab} and θ_{ba}.

Using the computer algebra package Mathcad (Mathsoft 2001) we can eliminate M_1, M_2, θ_1 and θ_2 to produce the following equations:

$$M_{ab} = i_1\nu_1 \frac{(k_{splice}[\cos(\nu_1)\cos(\nu_2)i_2\nu_2 - \sin(\nu_1)\sin(\nu_2)i_1\nu_1] - \nu_1\nu_2 i_1 i_2\cos(\nu_2)\sin(\nu_1))\theta_{ab} - k_{splice}i_2\nu_2\theta_{ba}}{\nu_1\nu_2 i_1 i_2\cos(\nu_1)\cos(\nu_2) + k_{splice}[i_1\nu_1\sin(\nu_2)\cos(\nu_1) + i_2\nu_2\sin(\nu_1)\cos(\nu_2)]} \tag{11}$$

$$M_{ba} = j\nu_2 \frac{(k_{splice}[\cos(\nu_1)\cos(\nu_2)i_1\nu_1 - \sin(\nu_1)\sin(\nu_2)i_2\nu_2] - \nu_1\nu_2 i_1 i_2\cos(\nu_1)\sin(\nu_2))\theta_{ba} - k_{splice}i_2\nu_2\theta_{ab}}{\nu_1\nu_2 i_1 i_2\cos(\nu_1)\cos(\nu_2) + k_{splice}[i_1\nu_1\sin(\nu_2)\cos(\nu_1) + i_2\nu_2\sin(\nu_1)\cos(\nu_2)]} \tag{12}$$

Eqs. (11) and (12) can be inserted into the column equations, whenever an element using a splice is encountered.

2.3. Special cases

Splices may appear at any point within a column element between the two beams which the element. The splices may be vary close to beam-column intersections and may also be treated as pinned points with zero stiffness. According to the FEM code (Federation Europeene de la Manutention, 2000) in the absence of experimental data for splices, all splices must be considered to be pinned connections in the column.

2.3.1. Splices at beam-column intersections

In this case we must consider separately the cases where the splice is placed at the top of the element below the beam-column intersection or at the bottom of the element above the beam-column intersection.

Considering the case of a splice which is attached to the bottom of an element, that is above a beam-column intersection, implies that the slope deflection equations, Eq. (3) and Eq. (4), are linked to the splice conditions, Eq. (9) and Eq. (10).

The revised splice conditions are

$$M_{ab} + M_2 = 0 \tag{13}$$

$$2k_{splice}(\theta_a - \theta_2) = M_2 - M_{ab} \tag{14}$$

In this case using Mathcad to eliminate θ_2 and M_2 we get the modified equations:

$$M_{ab} = k_{splice} i_2 v_2 \frac{\cos(v_2)\theta_{ab} - \theta_{ba}}{j v_2 \cos(v_2) + k_{splice}\sin(v_2)} \tag{15}$$

and

$$M_{ba} = i_2 v_2 \frac{(k_{splice}\cos(v_2) - i_2 v_1 \sin(v_1))\theta_{ab} - k_{splice}\theta_{ba}}{i_2 v_2 \cos(v_2) + k_{splice}\sin(v_2)} \tag{16}$$

These equations can also be derived directly from Eqs. (11) and (12) by setting the length L_1 to zero. The corresponding equations for the case where the splice is considered to be at the top of the element, immediately below the beam-column intersection, are

$$M_{ab} = i_1 v_1 \frac{(k_{splice}\cos(v_1) - i_1 v_1 \sin(v_1))\theta_{ab} - k_{splice}\theta_{ba}}{v_1 i_1 \cos(v_1) + k_{splice}\sin(v_1)} \tag{17}$$

and

$$M_{ba} = k_{splice} i_1 v_1 \frac{-\theta_{ab} + \cos(v_1)\theta_{ba}}{v_1 i_1 \cos(v_1) + k_{splice}\sin(v_1)} \tag{18}$$

This latter case produces a lower buckling load as shown in Example 2 below.

2.3.2. Pinned splices

In the case of a pinned splice, Eq. (9) becomes

$$M_1 = M_2 = 0 \tag{19}$$

Hence the corresponding formulae for zero stiffness splices (effectively pinned connections in the middle of an element) are

$$M_{ab} = -i_1 v_1 \tan(v_1)\theta_{ab} \tag{20}$$

and

$$M_{ba} = -i_2 v_2 \tan(v_2)\theta_{ba} \tag{21}$$

Pinned splices just above, or just below, a beam-column intersection can be obtained by using Eq. (20) and Eq. (21) in combination with Eq. (19). For example, a pinned splice just above a beam column intersection leads to

$$M_{ab} = 0 \tag{22}$$

M_{ba} is given by Eq. (21).

3. Determination of the buckling load

3.1. Global equations

Fig. 7 shows the relationship between each element. The axial load acting on any element is the sum of the axial loads applied on each element above so that

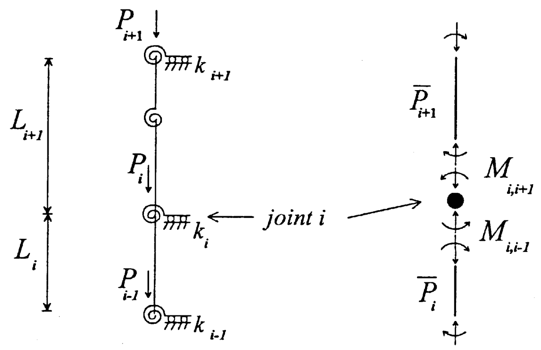

Fig. 7 Compatibility and element equilibrium

$$\overline{P}_i = \sum_{j=i}^{n} P_j \tag{23}$$

Moment equilibrium at a joint between beam and upright implies that

$$M_{i,\,i+1} + M_{i,\,i-1} = -k_i\theta_i \tag{24}$$

as the two column elements have the same rotation θ_i at the connection.

The moment equilibrium equation is reduced to

$$M_{0,\,1} = -k_0\theta_0 \tag{25}$$

at the bottom of the column, and

$$M_{n,\,n-1} = -k_n\theta_n \tag{26}$$

at the top of the column (level n).

Using Eq. (19) with the appropriate set of moment equations (3,4) or (11,12), etc. depending on the existence and the type of a splice in a given column element a tri-diagonal equation at node i of the form

$$c_{i,\,i-1}\theta_{i-1} + c_{i,\,i}\theta_i + c_{i,\,i+1} = 0 \tag{27}$$

can be obtained.

Summing up Eqs. (23)-(27) the following set of equations is derived:

$$[C]\{\theta\} = 0 \tag{28}$$

where $\{\theta\}^T = \{\theta_0, \theta_1, \theta_2, \ldots, \theta_n\}$ and

$$\{C\} = \begin{bmatrix} c_{0,0} & c_{0,1} & & & & & \\ c_{1,0} & c_{1,1} & c_{1,2} & & & & \\ & & \vdots & & & & \\ & & c_{i,i-1} & c_{i,i} & c_{i,i+1} & & \\ & & & & \vdots & & \\ & & & & c_{n-1,\,n-2} & c_{n-1,\,n-1} & c_{n-1,\,n} \\ & & & & & c_{n,\,n-1} & c_{n,\,n} \end{bmatrix} \tag{29}$$

Eq. (27) is a homogeneous linear matrix equation. The non-trivial solution for θ_i corresponds to the buckling equation. Hence the buckling load P_{cr} is given by

$$\det[C]_{P = P_{cr}} = 0 \tag{30}$$

3.2. Buckling load algorithm

The coefficients of Eq. (29) are transcendental functions of the load P. Expanding Eq. (30) using the Gauss elimination procedure gives

$$\prod_{i=0}^{n} c^*_{i,i} = 0 \tag{31}$$

where
$$c^*_{i,i} = c_{i,i} - c_{i-1,i}\frac{c_{i,i-1}}{c_{i-1,i-1}} \quad (i = 1, 2, \ldots, n) \tag{32}$$

The equation has $n + 1$ roots representing the $n + 1$ buckling loads. However, only the fundamental mode is required for structural design. The critical buckling load of a fixed ended column is given by $(2\pi)^2 EI / L^2$. The fundamental critical load of the column must therefore satisfy the inequality

$$0 < P_{cr} \le \max\left\{\frac{(2\pi)^2 EI_i}{L_i^2}\right\} \quad (i = 1, 2, \ldots, n) \tag{33}$$

A fast algorithm to determine the buckling load is:

(i) Determine an upper bound to the critical load by finding the maximum value of Eq. (33) (called P_{crmax}).

(ii) Set P initially equal to P_{crmax} divided 1000 and evaluate the determinant, Eq. (31). Increase P in steps of $P_{crmax}/1000$ until a change in sign of the determinant is obtained.

(iii) Use the method of bisection to refine the buckling load to the required accuracy.

Due to the explicit solution given in Eqs. (31) and (32) the above method converges to the buckling load extremely quickly (less than 1 second). In addition, as the steps in the increments of load are small it is not necessary to use William and Wittrick's algorithm (William and Wittrick 1983) to see if any buckling modes are omitted. When used in a design program the buckling load results are an upper bound to the design capability of pallet racks (Beale and Godley 2002). In the authors' experience many practical racks fail due to a combination of non-linear P–Δ effects with material non-linearity at loads which are often not more than 70% of the buckling loads.

4. Examples

4.1. Example 1: A single column with three beam levels

The height to the first beam level was 1500 mm while the two other storey heights were 1200 mm each. Young's Modulus of Elasticity was taken to be 210000 N/mm^2. Each storey carried a load of 4000 N. The splice was placed 2 m from the ground. i.e. between the first and second beam levels as shown

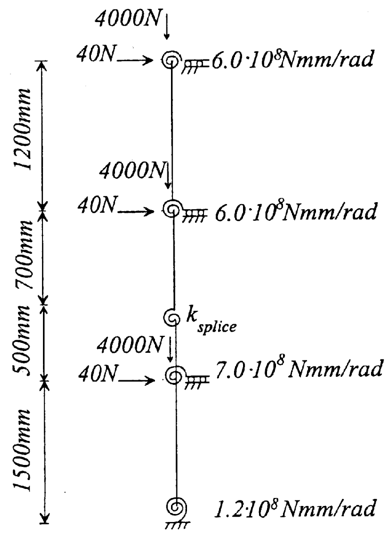

Fig. 8 Example 1

Table 1 Comparison of buckling load factors between Pallet and Lusas

k_{splice} Nmm/rad	pinned	$1.0 \cdot 10^6$	$1.0 \cdot 10^7$	$9.0 \cdot 10^7$	$5.0 \cdot 10^8$	Rigid
Pallet	7.087	7.135	7.396	7.683	7.737	7.750
Lusas	7.087	7.135	7.397	7.683	7.738	7.751

in Fig. 8. The base-plate/upright rotational stiffness was $1.2 \cdot 10^8$Nmm/rad. The second moment of area of the upright below the splice was taken to be 600000 mm^4 and of the upright above the splice to be 500000 mm^4. The beam-to-upright rotational stiffness was $7.0 \cdot 10^8$Nmm/rad below the splice and was $6.0 \cdot 10^8$Nmm/rad above the splice.

Note that although the same beam would normally be used throughout a pallet rack that the structural characteristics of the beam-end connector depend upon the upright to which it is connected, as well as to the beam, to which it is fitted. In many cases smaller uprights are used above splices and hence the rotational stiffnesses above and below the splice are generally different.

The rotational stiffness of the splice, called k_{splice} in Fig. 8 was varied from 0 Nmm/rad to $1.0 \cdot 10^8$ Nmm/rad covering the full range of splice conditions from a pinned to a rigid one. The buckling load factors obtained from the analysis are presented in Table 1. The program is called Pallet. The results are compared with a finite element solution obtained using the LUSAS program (FEA Ltd, 2001) and show excellent agreement. The finite element solution used 10 equally spaced Kirchoff thin beam elements for each column section along with joint elements at the base-plate, at each-beam-column intersection and at the splice. In addition constraint equations were used to enforce conditions of zero horizontal or vertical displacement at each joint position. There were a total of 40 beam elements, 5 joint elements and 10 constraint equations. The Pallet program used 3 elements to achieve the same results.

Fig. 9 shows the variation in elastic critical load with splice stiffness for this column. It can be clearly seen that different stiffnesses have a significant effect only for a limited range of splice stiffnesses. For a rotational stiffness less than 20000 Nmm/rad the splice may be considered as a pinned one, while for a rotational stiffness above $5.0 \cdot 10^8$Nmm/rad the connection is effectively rigid.

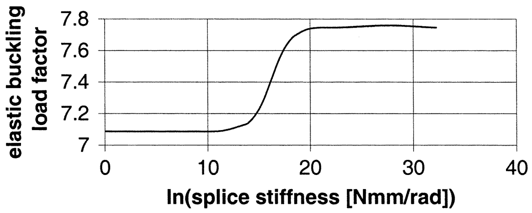

Fig. 9 Variation of elastic buckling load factor with splice stiffness

4.2. Example 2: Effects of splice near to beam level

To investigate the effects on buckling load factors of splices near to beam levels the position of the splice in Example 1 was considered to be either just above, or just below, the first beam level. In this case the stiffness of the splice was $1.0 \cdot 10^6$Nmm/rad. The program was able to smoothly converge to the limiting values as the splice moved closer to the beam level. The values of the limiting buckling load factors are shown in Table 2.

The excellent agreement between the two programs is shown by the results showing the influence of a weaker beam-column connection when the splice is below the beam level. Note that the difference in buckling loads between the two positions is shown for a relatively weak splice. If the splice had more typical values - in the order of $5.0 \cdot 10^7$ Nmm/rad - the difference between the buckling loads would be smaller. The program assumes that splices and beam-column connections are infinitesimally small. In practice, however, they have a finite size, typically in the range of 200-300 mm. For design purposes a splice should always be joined to the heavier section to get the increased performance that the designer is probably expecting.

Table 2 Influence of splice position on buckling load factor

	Below beam level	Above beam level
Pallet	4.4915	6.1420
Lusas	4.4912	6.1419

4.3. Example 3: Frame example

Fig. 10 shows a typical pallet rack frame with a splice at mid-height with the following data:

Second moment of area of the column sections below the splice is $7.0 \cdot 10^5$ mm^4
Second moment of area of the column sections above the splice is $6.0 \cdot 10^5$ mm^4.
Second moment of area of the beam sections is $5.5 \cdot 10^5$ mm^4.
Young's Modulus of Elasticity is $2.1 \cdot 10^5$N/mm^2.
The base-plate rotational stiffness is $9.0 \cdot 10^7$Nmm/rad.
The beam-column rotational stiffness is $7.0 \cdot 10^7$Nmm/rad below the splice
The beam-column rotational stiffness is $5.0 \cdot 10^7$Nmm/rad above the splice.
The rotational stiffness of the splice is $8.0 \cdot 10^7$Nmm/rad.

Note that although the same beam is used above and below the splice, that as different upright sections have been used then the beam-end connector has different structural properties above and below the splice.

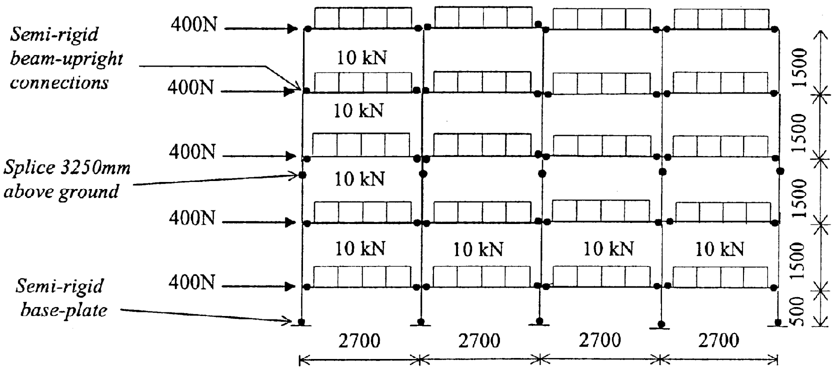

Fig. 10 Example frame

This pallet rack frame is similar to a frame without splices analysed by Davies (1992) and analysed by the authors (Feng *et al.* 1993). The two analyses showed excellent agreement.

Using Eq. (1), the equivalent beam-upright rotational stiffness is

$$\frac{1}{\dfrac{2700}{12 \cdot 210000 \cdot 5.5 \cdot 10^5} + \dfrac{1}{4.7 \cdot 10^7} + \dfrac{1}{4.7 \cdot 10^7}} = 1.10 \cdot 10^8 \text{ Nmm/rad}$$

below the splice and

$$\frac{1}{\dfrac{2700}{12 \cdot 210000 \cdot 5.5 \cdot 10^5} + \dfrac{1}{4.5 \cdot 10^7} + \dfrac{1}{4.5 \cdot 10^7}} = 8.36957 \cdot 10^7 \text{ mm/rad}$$

above it.

The structure consists of five uprights with corresponding base-plates, forming 4 bays. Therefore the effective second moment of area of a single column in the model is given by $(5/4) \cdot 7 \cdot 10^5$ mm^4= $8.75 \cdot 10^5$ mm^4 below the splice and $(5/4) \cdot 6 \cdot 10^5$ mm^4=$7.5 \cdot 10^5$ mm^4 above it.

Similarly, as there are 5 base-plates, the effective base-plate stiffness is given by $(5/4) \cdot 9.0 \cdot 10^7$ Nmm/rad=$1.125 \cdot 10^8$ Nmm/rad.

For each one of the 5 splices the effective stiffness is $(5/4) \cdot 8.0 \cdot 10^7$=$1.0 \cdot 10^8$ Nmm/rad.

The buckling load factor from the Pallet program was 2.554 and from a finite element analysis using Lusas was 2.539. The difference, being only 0.6%, is within the error margin of the finite element method. The finite element model of the frame used 10 equally spaced Kirchoff thin beam elements for each beam and 10 equally spaced beam elements per section of upright. In addition at the end of every beam, at each splice and at each base-plate a rotational joint element was included giving a total of 555 elements. Constraint equations were also used at each joint position to enforce conditions of no horizontal or vertical displacement between the ends of the joint. There were 100 constraint equations. The Pallet program required 5 elements only, one for each section of upright. Fig. 11 shows a plot obtained from the finite element program of the first, fundamental mode of buckling of the rack clearly showing a sway failure in accordance with the assumptions made in the paper.

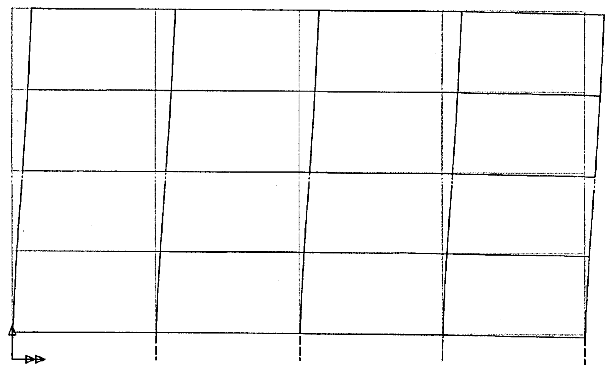

Fig. 11 Lowest elastic buckling mode of example frame

5. Conclusions

The paper has developed an efficient procedure for the analysis of pallet racks containing splices. Although not presented here in the examples, the method is capable of analysing frames containing several splices.

The position of splices close to beam-column intersections has been proven to have a significant influence on the fundamental buckling load of spliced pallet racks.

The use of a computer algebra package has been shown to be an efficient procedure in the derivation of element stiffness matrices enabling complex algebraic manipulations to be easily carried out. It also enabled the derivation of stiffness matrices for the special cases of zero stiffness splices and splices close to beam-column intersections.

References

Beale, R.G. and Godley, M.H.R. (2001), "Problems arising with pallet rack semi-rigid base-plates", *Proc. 1st Int. Conf. On Steel & Composite Structures*, Pusan, 699-706.

Beale R.G. and Godley M.H.R. (2002), "The design of the pallet program", *Proc. 16th Int. Speciality Conf. on Cold-Formed Steel Structures*, Orlando, 353-368.

Davies, J.M. (1980), "Stabilities of unbraced pallet racks", *Proc. 5th Int. Speciality Conf. on Cold-Formed Steel Structures*, St. Louis, 409-428.

Davies, J.M. (1992), "Down-aisle stability of rack structures", *Proc. of 11th Int. Speciality Conf. on Cold-Formed Steel Structures*, St. Louis, 417-435.

FEA Ltd., (2000), "Lusas User Guide Version 13".

Federation Europeenne de la Manutention, Section X, (2000), *Recommendations for the Design of Steel Static Pallet Racking and Shelving*.

Feng, X., Godley, M.H.R. and Beale, R.G. (1993), "Elastic buckling analysis of pallet rack structures", *Developments in Structural Computing*, Edinburgh, 207-305.

Godley, M.H.R., Beale, R.G. and Feng, X. (1998), "Rotational stiffnesses of semi-rigid base-plates", *Proc. 14th Int. Speciality Conf. on Cold-Formed Steel Structures*, St. Louis, 323-334.

Godley, M.H.R., Beale, R.G. and Feng, X. (2000), "Analysis and design of down-aisle pallet rack structures", *Comp. Struct.*, **77**(4), 391-401.

Horne, M.R. and Merchant, W. (1965), *The Stability of Frames*, Pergamon.

Lewis, G.M. (1991), "Stability of rack structures", *Thin-Walled Struct.*, **27**, 163-174.
Markazi, F., Godley, M.H.R. and Beale, R.G. (1997), "Experimental analysis of semi-rigid boltless connections", *Thin-Walled Struct.* **27**, 53-87.
Mathsoft Inc, (2001), "Mathcad User's Guide with Reference Manual".
McConnel. R.E. and Kelly, S.J. (1983), "Structural aspects of the progressive collapse of warehouse racking", *The Struct. Eng.* **48**(11), 343-347.
Williams, F.W. and Wittrick, W.H. (1983), "Exact buckling and frequency calculations surveyed", *J. Struct. Eng.*, **109**(1), 169-187.
Yu, W-W. (1973), *Cold-Formed Structures*, McGraw-Hill.

Notation

$c_{i,j}$	: element *i,j* of stiffness equation
i	: joint number
i_{ab}	: EI/L
i_1	: EI_1/L_1
i_2	: $EI_2/(L - L_1)$
k_0	: rotational stiffness of the semi-rigid upright-base-plate
k_i	: rotational stiffnesses of beam-to-upright joints
k_{li}	: rotational stiffness of left-hand beam-to-upright joint
k_{ri}	: rotational stiffness of right-hand beam-to-upright joint
k_{splice}	: rotational stiffness of a splice
l	: width of each bay
E	: Young's Modulus of Elasticity
I	: second moment of area of column element
I_{bi}	: second moment of area of the beam at level *a*
L	: length of column element
L_1	: length of column element below splice
M_{ab}	: bending moment at node *a* of element *ab*
M_{ba}	: bending moment at node *b* of element *ab*
M_1	: bending moment below splice
M_2	: bending moment above splice
P	: axial load within column element
$\overline{P}_i$	: total axial load acting on column element
P_{cr}	: elastic buckling load of rack
θ_a	: rotation of node *a*
θ_b	: rotation of node *b*
θ_1	: rotation of column element below splice
θ_2	: rotation of column element above splice
ν	: $\sqrt{\frac{P}{EI}}L$
ν_1	: $\sqrt{\frac{P}{EI_1}}L_1$
ν_2	: $\sqrt{\frac{P}{EI_2}}(L-L_1)$

CC